Lattice-parameter variation with carbon content of martensite. II. Long-wavelength theory of the cubic-to-tetragonal transition

Zhong Fan, Liu Xiao, and Zhang Jinxiu
Department of Physics, Zhongshan University, Guangzhou, 510275, People's Republic of China

Kang Mokuang and Guo Zhenqi
Department of Material Science and Engineering, Northwestern Polytechnic University, Xian, 710072, People's Republic of China
(Received 7 February 1995)

Based on the experimental observation of cubic-to-tetragonal transition of low-carbon martensite, we perform a long-wavelength approximation for the stress-induced elastic interaction in the theory of microscopic elasticity. Taking into account the elastic anisotropy and the tetragonal character of the octahedral interstices in α-iron, we consistently obtain the cubic-to-tetragonal transition of first-order nature at the carbon concentration of 0.18 wt %, using the order-disorder transition theory formulated by Khachaturyan with the method of static concentration waves. The detailed variation of the lattice parameters and axial ratio is also given compatibly with our results. The difference in experimental results between single crystals and polycrystals is emphasized, and a phenomenological two-dimensional internal strain is proposed to explain the transition in thin-plate samples. The results are in good agreement with experimental observations.

I. INTRODUCTION

It was found[1] and later confirmed[2,3] long ago that, for plain carbon steels and even alloyed steels,[4,5] the lattice parameters of the body-centered tetragonal martensite are determined by the carbon content of the initial austenite as

$$a = a_0 - \beta\rho \ , \tag{1.1a}$$

$$c = a_0 + \alpha\rho \ , \tag{1.1b}$$

and

$$c/a = 1 + \gamma\rho \ , \tag{1.1c}$$

where a_0 is the bcc α-iron lattice parameter, ρ the weight percent of carbon, and

$$\alpha = 0.116 \pm 0.002 \text{ Å}, \quad \beta = 0.013 \pm 0.002 \text{ Å} \ ,$$

and

$$\gamma = 0.046 \pm 0.001 \ . \tag{1.2}$$

This concentration dependence of the lattice parameters is one of the most important experimental proofs of the facts that martensite is a supersaturated solid solution of carbon in α-iron, and that the mechanism of the transformation is a diffusionless homogeneous deformation[6,7] from fcc γ-austenite, such that the carbon atoms, occupying the octahedral interstitial sites of the γ lattice, fall into only the O_z sublattice of the α-iron. The α lattice has three octahedral interstitial sublattices O_x, O_y, and O_z, displaced from the origin by the vectors $\mathbf{h}_1 = (\frac{1}{2},0,0)$, $\mathbf{h}_2 = (0,\frac{1}{2},0)$, and $\mathbf{h}_3 = (0,0,\frac{1}{2})$, respectively. If carbon atoms occupy the three sublattices uniformly, the resulting lattice is cubic. The preferential occupation of one of the three sublattices can be viewed as an ordered distribution of carbon atoms in them. This leads to the tetragonality of the resulting lattice. Later experiments at abnormally low[8–13] and high[14–18] axial ratio c/a and determination of its variation in freshly formed and subsequently heated martensites have revealed that the ordered distribution is a thermodynamically more stable state than the disordered one, instead of merely an effect of a diffusionless transformation. The neutron diffraction results,[19] on the other hand, indicate that the normal axial ratio, Eq. (1.1c), corresponds to an only partially ordered state, i.e., only about 80% of carbon atoms occupy the O_z sublattice. The abnormal cases and their variation with temperature arise from the nonequilibrium distribution of carbon atoms in as-quenched martensites.

Theoretically, Zener[20] suggested in 1946 that the ordered distribution resulted from stress-induced interaction of the carbon atoms. Thus there exists a critical carbon concentration (or temperature) at a definite temperature (or concentration) above (or below) which ordering appears because the resulting reduction in elastic energy dominates the decrease in entropy, hence leading to a decrease, instead of an increase,[21] in free energy; this is the basic mechanism of phase transitions. Accordingly, he found the cubic-tetragonal transition occurred at about 0.6 wt % carbon at room temperature. Taking into account the discrete structure of the crystal lattice and elastic anisotropy as well as the fact that each interstitial atom is a center of tetragonal deformation, Kurdjumov and Khachaturyan[22] later used a self-consistent theory of the order-disorder transition with static concentration waves[23] and microscopic elasticity theory[24–26] to obtain a similar result. However, the experimental results of partially rather than completely ordered distribution of carbon atoms led to considerably higher values of the distor-

tion of the iron lattice and hence concentration coefficients of linear expansion $u_{ij}(p)$. Consequently, they revised their calculation of elastic interaction energy, reducing the critical carbon concentration for ordering at room temperature to 0.18 wt %.[27,28] This value is in better agreement with the fact that carbon martensite with a cubic lattice had not been experimentally observed[22] until the work of Liu *et al.*[29] (hereafter referred to as I).

Utilizing thin-foil samples to release internal stresses, we have experimentally observed cubic martensites in I. A transition from a cubic to a tetragonal lattice near 0.2 wt % carbon has also been confirmed by the variation of the {200} peak of x-ray diffraction. These results led to the present careful reexamination of the previous theories of the order-disorder transition of carbon atoms in martensite. We arrive at a similar critical carbon concentration of 0.18 wt %, by using a long-wavelength approximation to the stress-induced interaction to account for the low concentration of carbon, thus removing several inconsistencies in the previous theories (Sec. III). We also give detailed theoretical curves of the lattice parameters versus carbon concentration from zero, since Eqs. (1.1) are obtained only from high concentrations, and the usual extrapolation erroneously excludes cubic martensite.

We review briefly the previous theories in Sec. II to collect the relevant formula, and then present a detailed analysis in Sec. III. Section IV contains a phenomenological theory for comparison with experiment. Section V concludes with a discussion.

II. REVIEW OF THE THEORIES

We shall briefly review the theories of order-disorder transitions and microelasticity and the relations between lattice parameters and carbon concentration, following the method formulated by Khachaturyan and Shatalov.[30,31]

A. Order-disorder transition

The distribution of carbon atoms in the three sublattices of interstices can be viewed as the arrangement of a binary substitutional solution of carbon atoms and vacancies, and is described by the occupation probability $n(p,\mathbf{R})$ of finding an atom at an interstice $\mathbf{r}=\mathbf{R}+\mathbf{h}_p$, where $\mathbf{R}$ are the coordinates of the unit cell and $p=1$, 2, and 3 represents the three sublattices. The atomic structure can be further represented as a linear superposition of the static concentration waves

$$u_\sigma(\mathbf{k},p,\mathbf{R})=v_\sigma(\mathbf{k},p)e^{i\mathbf{k}\cdot\mathbf{R}} \tag{2.1}$$

where $\mathbf{k}$ is the wave vector, σ the polarization number, and $v_\sigma(\mathbf{k},p)$ is a unit polarization vector characterizing the contribution of a concentration wave $(\sigma,\mathbf{k})$ to the atomic distribution in the pth sublattice. Thus

$$n(p,\mathbf{R})=\frac{C}{3}+\sum_{\sigma,s} z_{\sigma,s}\varepsilon_{\sigma,s}(p,\mathbf{R}) , \tag{2.2a}$$

where

$$\varepsilon_{\sigma,s}(p,\mathbf{R})=\tfrac{1}{2}\sum_{j_s}[\gamma_\sigma(j_s)v_\sigma(\mathbf{k}_{j_s},p)e^{i\mathbf{k}_{j_s}\cdot\mathbf{R}}+\text{c.c.}] , \tag{2.2b}$$

where C is the atomic concentration of carbon atoms, j_s runs over the vectors of the star s, $z_{\sigma,s}$ is the long-range order parameter, and $\gamma_\sigma(j_s)$ a coefficient determining the superlattice symmetry with respect to rotation and reflection.

The static concentration waves can be chosen as the eigenvectors of the pairwise interaction matrix $\mathbf{W}_{pq}(\mathbf{R})$ characterizing the interaction of two atoms at the p and q interstices in two unit cells separated by $\mathbf{R}$, i.e.,

$$\sum_{q,R'} W_{pq}(\mathbf{R}-\mathbf{R}')u_\sigma(\mathbf{k},q,\mathbf{R}')=\lambda_\sigma(\mathbf{k})u_\sigma(\mathbf{k},p,\mathbf{R}) , \tag{2.3}$$

or in Fourier transform

$$\sum_{q=1}^{3} V_{pq}(\mathbf{k})v_\sigma(\mathbf{k},q)=\lambda_\sigma(\mathbf{k})v_\sigma(\mathbf{k},p), \quad \sigma=1,2,3 , \tag{2.4}$$

where

$$V_{pq}(\mathbf{k})=\sum_R W_{pq}(\mathbf{R})e^{i\mathbf{k}\cdot\mathbf{R}} . \tag{2.5}$$

since $V_{pq}(\mathbf{k})$ is a Hermitian matrix, all the eigenvalues $\lambda_\sigma(\mathbf{k})$ are real and their eigenvectors $v_\sigma(\mathbf{k},q)$ form an orthonormal and complete set of functions.

The equilibrium distribution can be found self-consistently by noting that each lattice site of the three sublattices can only be occupied by one or zero of the atoms of some definite type. Accordingly,

$$n(p,\mathbf{R})=\left[\exp\left\{-\beta\left[\mu-\sum_{q,R'} W_{pq}(\mathbf{R}-\mathbf{R}')\times n(q,\mathbf{R}')\right]\right\}+1\right]^{-1} , \tag{2.6}$$

where $\beta=1/k_BT$, μ is the chemical potential determined by the total number of interstitial atoms, and k_B is the Boltzmann constant. The solution $n(p,\mathbf{R})$ of this equation provides the extrema of the Helmholtz free energy

$$F=\tfrac{1}{2}\sum_{p,q}\sum_{R,R'} W_{pq}(\mathbf{R}-\mathbf{R}')n(p,\mathbf{R})n(q,\mathbf{R}') + k_BT\sum_{p,R}\{n(p,\mathbf{R})\ln[n(p,\mathbf{R})] + [1-n(p,\mathbf{R})]\ln[1-n(p,\mathbf{R})]\} . \tag{2.7}$$

By linearizing Eq. (2.6) at $C/3$ corresponding to the disordered cubic state, the ordering temperature of the most stable high-temperature ordered phase can be obtained as

$$T_c=-\frac{C}{3k_B}\left[1-\frac{C}{3}\right]\lambda_{\sigma_0}(\mathbf{k}_{s_0}) , \tag{2.8}$$

where $\lambda_{\sigma_0}(\mathbf{k}_{s_0})$ is the absolute minimum of all $\lambda_\sigma(\mathbf{k})$. Ac-

cordingly, the structure of the ordered phase can be obtained based on the star s_0 and the polarization σ_0.

B. Stress-induced pairwise interaction matrix

The stress-induced interaction of two atoms has been formulated in Ref. 24 and in Refs. 25 and 26, which give[30]

$$V_{pq}(\mathbf{k})=\begin{cases}-v_0\lambda_{ijkl}u_{ij}(p)u_{kl}(q)+Q_{pq} & \text{for } \mathbf{k}=\mathbf{0} \quad (2.9a)\\ -F_i(p,\mathbf{k})G_{ij}(\mathbf{k})F_j^*(q,\mathbf{k})+Q_{pq} & \text{for } \mathbf{k}\neq\mathbf{0} \quad (2.9b)\end{cases}$$

with

$$Q_{pq}=\frac{1}{N}\sum_{k}F_i(p,\mathbf{k})G_{ij}(\mathbf{k})F_j^*(q,\mathbf{k}) . \quad (2.10)$$

Here λ_{ijkl} is the elastic modulus tensor, v_0 the atomic volume equal to $a_0^3/2$ for the bcc lattice, with a_0 the iron lattice parameter, N is the total number of iron atoms, and $F_i(p,\mathbf{k})$ is the Fourier transform of the Kanzaki force[32] $f_i(p,\mathbf{R}-\mathbf{R}')$, with which the solute atom $(p,\mathbf{R})$ acts on a host atom at site $\mathbf{R}'$ of the undistorted host lattice $G_{ij}(\mathbf{k})$ is the Green's tensor that is the inverse of the dynamic matrix determining the vibrational frequency spectrum of a crystal. Repeated subscripts always imply summation unless otherwise indicated. Thus it is clear that $V_{pq}(\mathbf{k})$ is the interaction between two solute atoms mediated by the lattice displacement.

C. Relations between lattice parameters and carbon concentration

To relate the theory to the experimentally observed dependence of the lattice parameters on carbon concentration, assume that the occupation fractions of the interstices O_x, O_y, and O_z are n_1, n_2, and n_3, respectively, with

$$n_1+n_2+n_3=C . \quad (2.11)$$

The resulting crystal lattice distortion is

$$\bar{u}_{ij}=u_{ij}(1)n_1+u_{ij}(1)n_2+u_{ij}(1)n_3 . \quad (2.12)$$

The tetragonal uniform strains produced by the insertion of interstitial atoms are

$$u_{ij}(1)=\begin{bmatrix}u_{33}^0 & 0 & 0\\ 0 & u_{11}^0 & 0\\ 0 & 0 & u_{11}^0\end{bmatrix},$$

$$u_{ij}(2)=\begin{bmatrix}u_{11}^0 & 0 & 0\\ 0 & u_{33}^0 & 0\\ 0 & 0 & u_{11}^0\end{bmatrix}, \quad (2.13)$$

$$u_{ij}(3)=\begin{bmatrix}u_{11}^0 & 0 & 0\\ 0 & u_{11}^0 & 0\\ 0 & 0 & u_{33}^0\end{bmatrix}.$$

This distortion transforms the bcc host lattice into the orthorhombic one with unit translations[30]

$$a=a_0[1+u_{11}^0(n_2+n_3)+u_{33}^0n_1] , \quad (2.14a)$$

$$b=a_0[1+u_{11}^0(n_1+n_3)+u_{33}^0n_2] , \quad (2.14b)$$

$$c=a_0[1+u_{11}^0(n_1+n_2)+u_{33}^0n_3] . \quad (2.14c)$$

III. LONG-WAVELENGTH THEORY

A. Theory

In the previous calculation of ordering,[22,27,28] one used the nearest- and next-nearest-neighbor, i.e., short-range, interactions directly to obtain $V_{pq}(\mathbf{k})$. This obviously contradicts the results corresponding to a dilute solution. For a carbon concentration of, say, 1 at. % or 0.22 wt %, there is, on average, only one carbon atom among 50 unit cells. Thus it is clear that the interaction should be calculated in the long-range limit. Another omission in the previous theories is the p and q dependence of Q. Although crystallographically the three sublattices are equivalent, the interaction between two atoms with $p=q$ and $p\neq q$ is obviously different, owing to the tetragonal symmetry of the octahedral interstices. A correct calculation should therefore be based on the continuum limit of $V_{pq}(\mathbf{k})$, or specifically F_i and G_{ij}. This has been performed in Ref. 30 in the case of an isotropic medium.

By keeping the first nonvanishing terms of the Taylor expansions and replacing the summation over N points of the first Brillouin zone by an integration over a sphere with equal volume $(2\pi)^3/v_0$, one has[30]

$$L_{pq}(\mathbf{n})\equiv F_i(p,\mathbf{k})G_{ij}(\mathbf{k})F_j^*(q,\mathbf{k})$$
$$=-v_0\sigma_{il}(p)n_l\Omega_{ij}(\mathbf{n})n_k\sigma_{jk}(q) , \quad (3.1)$$

$$Q_{pq}=\langle L_{pq}(\mathbf{n})\rangle , \quad (3.2)$$

$$V_{pq}(\mathbf{k})=-L_{pq}(\mathbf{n})+\langle L_{pq}(\mathbf{n})\rangle , \quad (3.3)$$

with

$$\sigma_{ij}(p)=\lambda_{ijkl}u_{kl}(p) , \quad (3.4)$$

$$\Omega_{ij}^{-1}(\mathbf{n})=\lambda_{ijkl}n_kn_l , \quad (3.5)$$

where the average is over all directions of the vector $\mathbf{n}=\mathbf{k}/|\mathbf{k}|$.

For a cubic medium,

$$\lambda_{1111}=\lambda_{2222}=\lambda_{3333}=C_{11} , \quad (3.6a)$$

$$\lambda_{1122}=\lambda_{1133}=\lambda_{2233}=C_{12} , \quad (3.6b)$$

$$\lambda_{1212}=\lambda_{1313}=\lambda_{2323}=C_{44} , \quad (3.6c)$$

we have, from Eq. (3.5),

$$\Omega_{ii}^{-1}(\mathbf{n})=C_{44}+(C_{11}-C_{44})n_i^2 , \quad (3.7a)$$

$$\Omega_{ij}^{-1}(\mathbf{n})=(C_{12}+C_{44})n_in_j . \quad (3.7b)$$

Hence the inverse components are

$$\Omega_{ii}(\mathbf{n})=\frac{1}{c_{44}D(n)}[C_{44}+(C_{11}-C_{44})(n_j^2+n_k^2)+\xi(C_{11}+C_{12})n_j^2n_k^2]\ , \tag{3.8a}$$

$$\Omega_{ij}(\mathbf{n})=-\frac{1}{c_{44}D(n)}(C_{12}+C_{44})(1+\xi n_k^2)n_in_j\ , \tag{3.8b}$$

with

$$D(\mathbf{n})=C_{11}+(C_{11}+C_{12})\xi(n_1^2n_2^2+n_2^2n_3^2+n_3^2n_1^2)+\xi^2(C_{11}+2C_{12}+C_{44})n_1^2n_2^2n_3^2\ , \tag{3.9}$$

and

$$\xi=(C_{11}-C_{12}-2C_{44})/C_{44}\ , \tag{3.10}$$

where the indices i, j, and k form a cyclic sequence [summation over the repeated indices is not implied in Eqs. (3.7) and (3.8), which have also been obtained in Ref. 30 in a different context, though with some misprints.] Note that $\xi=0$ corresponds to an isotropic medium. Therefore, from Eqs. (3.2) and (3.4), we reach

$$Q_{pq}=v_0\sum_i\sigma_{ii}(p)\langle n_i\Omega_{ii}(\mathbf{n})n_i\rangle\sigma_{ii}(q)+v_0\sum_{i\neq j}\sigma_{ii}(p)\langle n_i\Omega_{ij}(\mathbf{n})n_j\rangle\sigma_{jj}(q)\ , \tag{3.11}$$

or specifically

$$Q_{11}=v_0\frac{(\sigma_{33}^0)^2+2(\sigma_{11}^0)^2}{c_{44}}q_1-v_0\frac{4\sigma_{33}^0\sigma_{11}^0+2(\sigma_{11}^0)^2}{c_{44}}q_2\ , \tag{3.12a}$$

$$Q_{12}=v_0\frac{2\sigma_{33}^0\sigma_{11}^0+(\sigma_{11}^0)^2}{c_{44}}q_1-v_0\frac{(\sigma_{33}^0)^2+2\sigma_{33}^0\sigma_{11}^0+3(\sigma_{11}^0)^2}{c_{44}}q_2\ , \tag{3.12b}$$

with

$$q_1=\langle[C_{44}+(C_{11}-C_{44})(n_1^2+n_2^2)+\xi(C_{11}+C_{12})n_1^2n_2^2]D(\mathbf{n})\rangle\ , \tag{3.13a}$$

$$q_2=\langle(C_{12}+C_{44})(1+\xi n_3^2)n_1^2n_2^2/D(\mathbf{n})\rangle\ , \tag{3.13b}$$

and

$$\sigma_{11}^0=(C_{11}+C_{12})u_{11}^0+C_{12}u_{33}^0\ , \tag{3.14a}$$

$$\sigma_{33}^0=2C_{12}u_{11}^0+C_{11}u_{33}^0\ . \tag{3.14b}$$

Having determined the elastic interaction matrix, we can then find its eigenvalues and associated eigenvectors. Note that, since we are concerned only with the long-wavelength approximation, $\mathbf{k}=\mathbf{0}$ is the only Lifshitz point which can result in a nonaccidental stable ordered phase. At $\mathbf{k}=\mathbf{0}$ the matrix $V_{pq}(0)$ always has, by symmetry, the form

$$V_{pq}(0)=\begin{bmatrix}V_{11}(0) & V_{12}(0) & V_{12}(0)\\ V_{12}(0) & V_{11}(0) & V_{12}(0)\\ V_{12}(0) & V_{12}(0) & V_{11}(0)\end{bmatrix} \tag{3.15}$$

and has two different eigenvalues

$$\lambda_1(0)=V_{11}(0)+2V_{12}(0)=-v_0(C_{11}+2C_{12})(2u_{11}^0+u_{33}^0)^2+Q_{11}+2Q_{12} \tag{3.16a}$$

and

$$\lambda_2(0)=V_{11}(0)-V_{12}(0)=-v_0(C_{11}-C_{12})(u_{11}^0-u_{33}^0)^2+Q_{11}-Q_{12}\ , \tag{3.16b}$$

corresponding to the eigenvectors

$$v_1(p,0)=(v_1(1,0),v_1(2,0),v_1(3,0))=\frac{1}{\sqrt{3}}(1,1,1) \tag{3.17a}$$

and

$$v_2(p,0)=\frac{1}{\sqrt{6}}(-1,-1,2)\ ,\qquad v_3(p,0)=\frac{1}{\sqrt{2}}(1,-1,0)\ , \tag{3.17b}$$

respectively, the last two being degenerate. From Eqs. (2.2), we have generally, for $\mathbf{k}=\mathbf{0}$,

$$n(p,\mathbf{R})=\frac{C}{3}+\sum_\sigma z_\sigma\gamma_\sigma v_\sigma(p,0)=\begin{cases}\dfrac{C}{3}+z\gamma_1v_1(p,0) & \text{for } \sigma=1\\ \dfrac{C}{3}+z_2\gamma_2v_2(p,0)+z_3\gamma_3v_3(p,0) & \text{for } \sigma=2,3\ .\end{cases} \tag{3.18}$$

Therefore only $\lambda_2(0)$ is associated with ordering: $\lambda_1(0)$ corresponds to a disordered state with carbon atoms populating the three interstitial sublattices equally. According to Eq. (2.8), ordering occurs only when $\lambda_2(0)<\lambda_1(0)$. We will see in Sec. III that this is not the case in Ref. 27, although the authors obtained ordering below 0.2 wt % carbon at room temperature. Their numerical results would have had $\lambda_1(0)<\lambda_2(0)$ so that no

ordering would have occurred, had they consistently considered $\lambda_1(0)$ as emphasized in Ref. 30.

Generally, from Eq. (3.18), the ordered state has three different values of $n(p,\mathbf{R})$, so that there are two long-range order parameters, consistent with the criterion for $n(p,\mathbf{R})$ being the solution of Eq. (2.6).[30] Thus the ordered state will be orthorhombic. As we are concerned here only with tetragonal martensite, we will only consider, for simplicity, $\sigma=2$, as in Ref. 27. $\sigma=3$ leads to a continuous transition to an orthorhombic phase at the temperature determined by Eq. (2.8), which is lower than the first-order transition temperature of $\sigma=2$.

Substituting Eq. (3.17b) into Eq. (3.18), we obtain the distributions

$$n(p,\mathbf{R})=\begin{cases}\frac{C}{3}(1-z) & \text{for } p=1 \text{ and } 2\\ \frac{C}{3}(1+2z) & \text{for } p=3,\end{cases} \tag{3.19}$$

where we have chosen $\gamma_2=\sqrt{6}C/3$ so that the completely ordered state has $z=1$. Applying this result to Eqs. (2.6) and (2.7), we get, after some manipulations, the dependence of the order parameter on temperature and concentration and the free energy, respectively, as

$$-\frac{k_BT}{C\lambda_2(0)}=\frac{z}{\ln[(1+2z)/(1-z)]} \tag{3.20}$$

and

$$F(T,C,z)=\tfrac{1}{6}NC^2\lambda_1(0)+Nk_BTC\ln\left[\frac{C}{3}\right]+\tfrac{1}{3}NC^2\lambda_2(0)z^2$$
$$+\tfrac{1}{3}Nk_BTC[(1+2z)\ln(1+2z)$$
$$+2(1-z)\ln(1-z)]\,, \tag{3.21}$$

in the limit of dilute solution, $C\ll 1$. These results can be cross-checked by noting that Eq. (3.20) gives the extrema of Eq. (3.21). The transition temperature, or concentration, instead of Eq. (2.8) with $\sigma_0=2$, the unstable point, is attained from Eq. (3.20) and $F(T,C,z)=F(T,C,0)$, or

$$-\frac{k_BT}{C\lambda_2(0)}=\frac{z^2}{(1+2z)\ln(1+2z)+2(1-z)\ln(1-z)}\,. \tag{3.22}$$

Finally the lattice parameters and the axial ratio can be obtained from Eqs. (2.14) and (3.19) as

$$a=b=a_0[1+\tfrac{1}{3}C(2u_{11}^0+u_{33}^0)-\tfrac{1}{3}Cz(u_{33}^0-u_{11}^0)]\,, \tag{3.23a}$$

$$c=a_0[1+\tfrac{1}{3}C(2u_{11}^0+u_{33}^0)+\tfrac{2}{3}Cz(u_{33}^0-u_{11}^0)]\,, \tag{3.23b}$$

$$c/a\approx 1+Cz(u_{33}^0-u_{11}^0) \tag{3.23c}$$

for $C\ll 1$.

B. Numerical results

Equations (3.9), (3.10), (3.12)–(3.14), (3.16), and (3.19)–(3.23) are the main formulas of the long-wavelength theory. In order to have quantitative results, we need to know the elastic constants C_{11}, C_{12}, and C_{44}, and a_0, u_{11}^0, and u_{33}^0. We use[29]

$$a_0=2.8664\ \text{Å}$$

and[27]

$$C_{11}=2.335\times10^{11}\ \text{N/m}^2,\quad C_{12}=1.355\times10^{11}\ \text{N/m}^2,$$
$$C_{44}=1.18\times10^{11}\ \text{N/m}^2\,. \tag{3.24}$$

As in Ref. 27, we assume that Eqs. (1.1) result from only 80% instead of 100% of carbon atoms occupying the O_z sublattice. From Eq. (3.19), $n_3=0.8C$ corresponds to an equilibrium order parameter $z=0.7$. Equating Eqs. (3.23a) and (3.23b) to Eqs. (1.1a) and (1.1b), respectively, with $z=0.7$, we obtain

$$u_{11}^0=-0.235\ \text{ and }\ u_{33}^0=1.143\,, \tag{3.25}$$

slightly different from Ref. 27 due to their different a_0 value.

To get the eigenvalues $\lambda_1(0)$ and $\lambda_2(0)$, we need to evaluate the directional average Eqs. (3.13). As $\mathbf{n}=(\sin\theta\cos\varphi,\sin\theta\sin\varphi,\cos\theta)$ and

$$\langle\cdot\rangle=\frac{1}{4\pi}\int_0^{\pi}\sin\theta\,d\theta\int_0^{2\pi}d\varphi\,\cdot\,,$$

q_1 and q_2 can be numerically integrated to be

$$q_1=0.342\ \text{ and }\ q_2=0.100\,. \tag{3.2b}$$

Consequently Eqs. (3.12) give

$$Q_{11}=6.755\ \text{eV}\ \text{ and }\ Q_{12}=1.724\ \text{eV}\,. \tag{3.27}$$

Thus Eqs. (3.16) lead to

$$\lambda_1(0)=-6.605\ \text{eV}\ \text{ and }\ \lambda_2(0)=-8.659\ \text{eV}\,. \tag{3.28}$$

Clearly, $\lambda_2(0)<\lambda_1(0)$. In Ref. 27, however, $Q_{pq}=Q\delta_{pq}$, and the interaction of the first few neighbors gives $Q=5.37$ eV. This in turn leads to $\lambda_1(0)=-11.44$ eV and $\lambda_2(0)=-8.32$ eV. The slight differences between our u_{11}^0 and u_{33}^0 and theirs cannot change the fact that in this case $\lambda_2(0)>\lambda_1(0)$, so that no ordering could actually occur in their theory. In Ref. 30, chemical contact repulsion due to overlap of electronic shells was taken into account to remove this discrepancy. Consequently, a critical concentration of 0.03 wt % was obtained. Such a low concentration, however, obviously cannot justify the short-range contact interaction.

Equation (3.20) leads to the variation of order parameter with the reduced parameter $\tau=-k_BT/C\lambda_2(0)$, as shown in Fig. 1. The point $\tau_c=\frac{1}{3}$, $z\to 0$ corresponds to T_c defined in Eq. (2.8) for $C\ll 1$. This point is associated with the instability of the disordered phase. By equating Eq. (3.20) to (3.22) to find the equilibrium order parameter $z_0=0.500$ at the transition point, the equilibrium

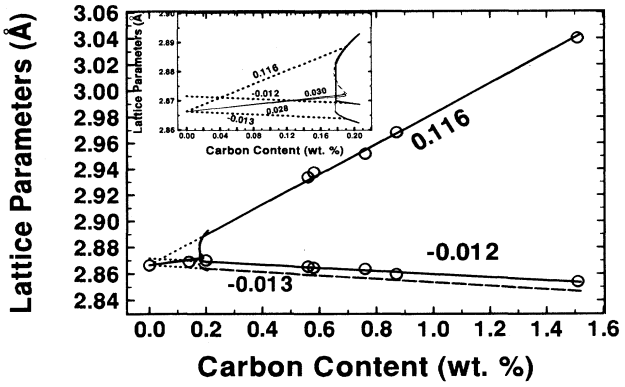

FIG. 1. Lattice parameters vs carbon content. Solid lines are theoretical lines, dotted ones are unphysical extrapolations. Circles are experimental points. Numbers indicate slopes. The inset shows the low-carbon-content portion of the figure.

phase boundary (T_0, C_0) can be obtained from Eq. (3.20) to be

$$\tau_0 = -\frac{k_B T_0}{C_0 \lambda_2(0)} = 0.361 > \tau_c \ . \tag{3.29}$$

Thus at the transition point there is a discontinuous jump of the order parameter from 0 to 0.500. The equilibrium relation, consequently, is the solid line in Fig. 1; the dashed one corresponds to the metastable and unstable states. Therefore the critical carbon concentration for the transition from cubically disordered to tetragonally ordered state at room temperature $T_0 = 300$ K is

$$C_0 = 0.000\,592 T_0 = 0.18 \text{ wt \%} \ . \tag{3.30}$$

At room temperature T_0, the dependence of order parameter on concentration is given by Eq. (3.20). For $C < C_0$, $z = 0$. Substituting these results into Eqs. (3.23), we obtain the variation of lattice parameters with carbon content, as also shown in Fig. 1, where the dashed lines also correspond to metastable and unstable states. At $C = C_0$, there are discontinuous jumps of a and c too. Note that the variation of a and c above C_0 with C also involves the variation of order parameter from z_0 to 1. For $z = 0.7$, α, β and $\gamma = 0.0450$ from Eqs. (3.23) are, of course, in agreement with Eq. (1.2).

IV. COMPARISON WITH EXPERIMENT

The theory above explains rather well the well-known relation between the lattice parameters and carbon content. It is based, however, on a stress-induced interaction that is derived without subjecting the material to external stress. Thus it can only apply to single crystals and powder samples, where internal stress can readily relax. For polycrystalline samples, the martensitic transformational strain and intergrain coordination will produce constraints on the elastic response of the medium, leading to deviation from the simple relation Eqs. (1.1). This is probably the main reason, in addition to the resolution of early experimental techniques, for the scatter in the experimental data along the line of Eqs. (1.1), as seen in the figure, for example, in Ref. 6. In fact, internal stress, arising from subsequent disordering and relating to the conjugation of the martensite and austenite lattices, has been invoked[22] to explain why cubic martensite has not been observed: It will qualitatively destroy the order-disorder transition by stabilizing the initial completely ordered state, which is assumed to have minimum elastic energy. This result, however, was obtained before the discovery of the fact that the freshly formed martensite in plain carbon steels is in a partly disordered state, and thus is questionable.

In our experiment, the samples used are thin (0.6 mm), compared to about 20 mm in the other two directions. Thus the internal stress in the direction perpendicular to the plate can readily relax. When ordering occurs, it is consequently favorable for the carbon atoms to line up in this direction, to be taken as the c axis. The a-b plane, on the other hand, is constrained so that it cannot completely follow the stress-free deformation. Thus, for a cubic martensite with low carbon content, the dilation of the lattice with addition of carbon atoms is constrained to counteract this effect, leading to a lower slope (0.02) as compared with the theoretical one (0.03). For the tetragonal martensite, on the other hand, the same effect reduces the contraction of the lattice to give a higher slope (-0.012) as compared with the theoretical value -0.013. This is quite reasonable albeit it is within the experimental error. Also the constraint causes an upward shift in the a axis.

As a quantitative explanation, we assume that a homogeneous additional internal strain exists in the a-b plane that is a function of the order parameter z and carbon concentration C, i.e.,

$$\Delta\varepsilon = \Delta\varepsilon(z, C) \ . \tag{4.1}$$

Accordingly the lattice parameters a and b become

$$a = b = a_0[1 + \tfrac{1}{3}C(2u^0_{11} + u^0_{33}) - \tfrac{1}{3}Cz(u^0_{33} - u^0_{11}) + \Delta\varepsilon(z, C)] \ . \tag{4.2}$$

Suppose that $\Delta\varepsilon$ is small, so that it can be expanded in its variables to the lowest order

$$\Delta\varepsilon = Az + BC \ , \tag{4.3}$$

where A and B are coefficients. This is reasonable as the higher z and C the larger the additional distortion, and hence the constant term is zero. Noting that $\Delta\varepsilon$ always counteracts the deformation of the a-b plane, we take B to be proportional to the change of a or b, or specifically

$$\Delta\varepsilon = Az - BC[(2u^0_{11} + u^0_{33}) - z(u^0_{33} - u^0_{11})] \ , \tag{4.4}$$

where we have made rearrangements of A and B in Eq. (4.3) to different ones with the same symbols. Thus

$$a = b = a_0[1 + Az + (\tfrac{1}{3} - B)C(2u^0_{11} + u^0_{33}) - (\tfrac{1}{3} - B)Cz(u^0_{33} - u^0_{11})] \ . \tag{4.5}$$

The additional internal strain gives rise to an additional elastic energy

$$\Delta E=\tfrac{1}{2}N\lambda(\Delta\varepsilon)^2=\tfrac{1}{2}N\lambda(A'^2z^2-2A'B'Cz+B'^2C^2)\ , \tag{4.6a}$$

where

$$A'=A+B(u_{33}^0-u_{11}^0)C\ , \tag{4.6b}$$

$$B'=B(2u_{11}^0+u_{33}^0)\ , \tag{4.6c}$$

and λ is a characteristic elastic energy. The total free energy is thus changed from Eq. (3.21) to

$$F'(T,C,z)=F(T,C,z)+\Delta E\ . \tag{4.7}$$

Accordingly, the equilibrium order parameter satisfies, by setting the first derivative of F' to zero,

$$-\left[C^2\lambda_2(0)+\frac{3\lambda A'^2}{2}\right]z+\frac{3\lambda A'B'}{2}C=Ck_BT\ln\frac{1+2z}{1-z}\ , \tag{4.8}$$

which returns to Eq. (3.20) when $A=B=0$. The corresponding relation to Eq. (3.22) is

$$-\left[C^2\lambda_2(0)+\frac{3\lambda A'^2}{2}\right]z^2+3\lambda A'B'zC=Ck_BT[(1+2z)\ln(1+2z)+2(1-z)\ln(1-z)]\ . \tag{4.9}$$

There are three parameters in the theory. A and B can be determined by fitting Eq. (4.5) to the experimental results. Suppose the ordered state also corresponds to an 80% occupation of the O_z sublattice, i.e., $z=0.7$. After the split of the {200} peak for $\rho>0.56$ wt % a is given experimentally by[29]

$$a=2.8716-0.012\rho\ . \tag{4.10}$$

Accordingly, from Eq. (3.25),

$$A=0.0026 \text{ and } B=0.028\ . \tag{4.11}$$

As an estimate of λ, we adopt the value of Ref. 22, which is 0.33 eV, although their additional strain is assumed to be proportional to $C(1-z)$. This value is obtained by supposing that the accommodation of the austenite and martensite lattices is accomplished by means of $(112)_M$ twinning.[22]

With these parameters, Eqs. (4.8) and (4.9) can be solved numerically. The results are shown in Fig. 2, where the curves with λ varying from 0 to 1 eV are also given for comparison. We note that as B always appears with C, a small concentration in the dilute case, as in Eq. (4.6b), it can be neglected compared with A. It is seen that the curves shift to a higher concentration as λ increases. However, this shift is quite small. Roughly, for $\lambda>0.1$, there is a small nonzero order parameter even when ρ is smaller than the transition point, the intersection point of Eqs. (4.8) and (4.9). This residual order parameter results from the internal-stressed-induced tetragonality. Nevertheless, even for $\lambda=1$ eV, the characteristic elastic energy v_0E, where E is a typical elastic constant, the ordering still persists due to the elastic interaction of the carbon atoms. This explains the experimental observation of the cubic-to-tetragonal transition. Lattice parameters are attained with the same procedures as previously and also shown in Fig. 1. The tetragonal axis c shifts slightly to a higher concentration; its slope, however, remains identical. Experimental points are also shown in the figure. The agreement with experiment is readily appreciated. It is worth mentioning that for low carbon content there is a slight tetragonality, with the slope of the a-C line being reduced from 0.030 to 0.028. We can, of course, choose B to compromise between the slopes of low high concentration, so that the low concentration one can be closer to the experimental value, 0.02. This, however, is trivial, as the experimental error for the low carbon content is larger, and self-tempering may also have an effect.

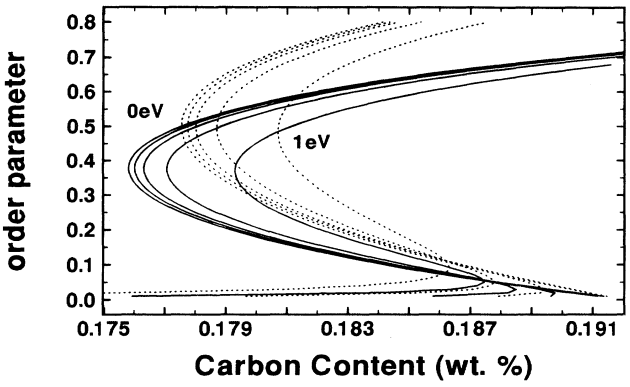

FIG. 2. Order parameter vs carbon content. Solid curves correspond to Eq. (4.8) and dotted ones to Eq. (4.9). The characteristic elastic energy λ is, from left to right, 0, 0.01, 0.1, 0.33, and 1 eV.

Figure 3 shows the dependence of the axial ratio on carbon concentration, both theoretically and experimentally. The axial ratio exhibits a reduction of 0.002 from 1, though with the same slope. This reduction results from the internal strain due to the accommodation of martensite and martensite or martensite and austenite. In carbon-free martensites, a reduction of similar magnitude (0.0025) has also been found,[33] which is also assumed to come from strain relaxation.

V. DISCUSSION

Though the tetragonality of ferrous martensites has long been established, there is still no consensus[21] as to whether it is an intrinsic transformation effect (consequence of the Bain distortion) or is the outcome of thermodynamic ordering. We note, as pointed out in the Introduction, that lowering of configurational entropy due

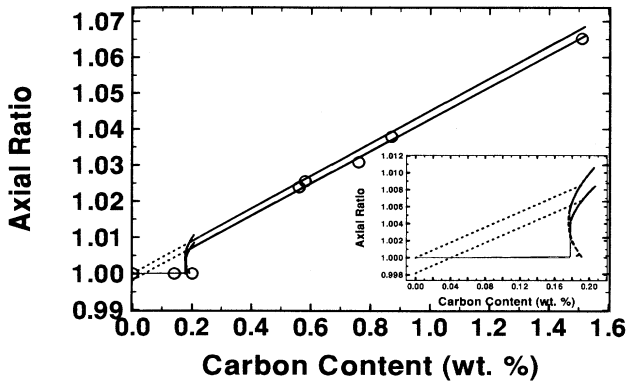

FIG. 3. Axial ratio vs carbon content. The lines and symbols have the same meaning as in Fig. 1.

to ordering cannot rule out the appearance of a thermodynamically ordered state. The main argument against the thermodynamic viewpoint, in our opinion, is that cubic martensite has never been observed.[22] Tetragonal martensite has been detected as carbon concentration as low as 0.2 wt %.[2] A small axial ratio, on the other hand, has been observed during decomposition of high-carbon martensite up to tempering temperatures of 200 °C and even up to 500 °C in alloyed steels.[34,35] This is, however, not unexpected, since martensite is a metastable product. Solid-solution decomposition, the long-wavelength concentration fluctuations of carbon atoms, for instance, occurs at temperatures near 100 °C and even at room temperature. Therefore it should be noted that the equilibrium used in the theory above is only relative; and the theory developed here concerns only the distribution of carbon atoms in the as-quenched state, where carbon atoms can be reasonably well approximated as uniformly distributed in the lattice as in the high-temperature disordered austenite. In I, cubic martensites have been observed only by varying the carbon content, instead of the temperature in the samples, and a transition to tetragonal martensite has also been observed accordingly. Taking into account the phenomena of abnormally high and low axial ratios discussed in Sec. I, we thus conclude that the tetragonality is thermodynamic in origin.

Developing a long-wavelength theory to account for the low carbon concentration near the transition, taking into account consistently the tetragonality of the distortion of the octahedral interstitials $[u_{ij}(p)]$ and the tetragonality of the stress-induced interaction (through Q_{pq}), we give a quantitative explanation of the transition and a detailed description of the resulting variation of the lattice parameters with respect to the carbon content, thus removing the apparent contradictions in the previous theories between the low content of carbon atoms and the short-range or even contact interaction among them. The transition is first order at the carbon concentration of 0.18 wt % at room temperature (300 K), with a discontinuous jump of order parameter of 0.50. Consequently, the lattice parameters and axial ratio also change abruptly at the transition point. We also address the difference in the measured lattice parameters and axial ratio between single-crystalline and polycrystalline samples, and accordingly we propose a phenomenological internal strain proportional to the order parameter and the carbon content, which gives an excellent fit to the experimental results and a qualitatively correct prediction for the reduction in slope of the *a-C* line in the cubic phase, but keeps the transition almost unchanged.

We have included in the theory the experimental outcome that only 80% of carbon atoms occupy the O_z interstice in freshly formed martensite in plain carbon steels. A question arises naturally: Why only 80%? We suggest that this is due to the stability of the host iron lattice with respect to the distortion resulting from the distribution of carbon atoms. In the theory of ordering considered here, only the interaction of carbon atoms is considered; the host lattice is assumed to withstand totally all the distortions. This is, of course, not always possible. Therefore some types of internal structural adjustment should take place. Theoretically, it is possible, at least in principle, to take into account the deformation of the host lattice to predict the stable range beyond which some adjustments occur. Experimentally, it has been found that[36] fresh martensites of Al and high-Ni carbon steels with abnormally high tetragonality have a platelike morphology with complete internal twinning, while normal or low-tetragonal martensites are mainly dislocated, so that carbon atoms are driven out by the strain field of the dislocations. We propose that this difference in morphology results from the self-accommodation of the host lattice to sustain the distortion of carbon distribution, and the abnormally high and low tetragonalities come from the stabilizing and unstabilizing effects of the alloyed elements on the lattice. It should be pointed out that this adjustment of the host lattice differs from the ordered transition of its interstitials: the basic structure remains intact. Experimental evidence is that the Mössbauer spectra remain unchanged after aging at 200 K, whereas the axial ratio diminishes remarkably.[37] Another example is the mechanism[38] of the additional $(011)_M$ twin proposed to find carbon atoms in the other two sublattices.

As the ordering of low-concentration interstitials has been observed in a number of interstitial solutions, we believe that many relevant phenomena can be explained by the theory developed in this paper, namely, the long-wavelength theory with due account of the internal stress and the distortion of the host lattice.

ACKNOWLEDGMENTS

X.L. acknowledges the support by the Advanced Research Foundation (Hong Kong) for Zhongshan University.

[1]G. V. Kurdjumov and E. Kaminsky, Nature **122**, 475 (1928); Z. Phys. **53**, 696 (1929).
[2]G. V. Kurdjumov, J. Iron Steel Inst. London **195**, 26 (1960).
[3]C. S. Roberts, Trans. Am. Inst. Metall. Eng. **197**, 203 (1953).
[4]Z. Nishiyama and M. Doi, J. Jpn. Inst. Met. **8**, 305 (1944).
[5]P. G. Winchell and M. Cohen, Trans. Am. Soc. Met. **55**, 347 (1962).
[6]E. Bain, Trans. Am. Inst. Metall. **9**, 751 (1924).
[7]G. V. Kurdjumov and G. Sachs, Z. Phys. **64**, 325 (1930).
[8]L. I. Lyssak and Ja. N. Vovk, Fiz. Met. Metalloved. **20**, 540 (1965).
[9]Ju. L. Alsehvsky and G. V. Kurdjumov, Fiz. Met. Metalloved. **22**, 730 (1966).
[10]Ju. L. Alshevsky, Fiz. Met. Metalloved. **27**, 716 (1969).
[11]L. I. Lyssak, Ja. N. Vovk and Ju. Polischuk, Fiz. Met. Metalloved. **23**, 898 (1967).
[12]L. I. Lyssak and L. O. Andrushchik, Fiz. Met. Metalloved. **28**, 348 (1969).
[13]L. I. Lyssak and V. E. Kanilchenko, Fiz. Met. Metalloved. **32**, 639 (1971).
[14]M. Watanabo and C. M. Wayman, Scr. Metall. **5**, 109 (1972).
[15]G. V. Kurdjumov, V. K. Kritskaya, and V. A. Ilina, Dokl. Akad. Nauk SSSR **219**, 1099 (1974) [Sov. Phys. Dokl. **19**, 850 (1975)].
[16]L. I. Lyssak, J. A. Artimiuk and Ju. M. Polishchuk, Fiz. Met. Metalloved. **35**, 1098 (1973).
[17]L. K. Mihailova, Dokl. Akad. Nauk SSSR **216**, 778 (1974) [Sov. Phys. Dokl. **19**, 371 (1974)].
[18]F. V. Kurdjumov, L. K. Mikhailova, and A. G. Khachaturyan, Dokl. Akad. Nauk SSSR **215**, 578 (1974) [Sov. Phys. Dokl. **18**, 159 (1974)].
[19]I. R. Entin, V. A. Somenkov and S. Sh. Shilstein, Dokl. Akad. Nauk SSSR **206**, 1096 (1972) [Sov. Phys. Dokl. **17**, 1021 (1973)].
[20]C. Zener, Trans. Am. Inst. Metall. Eng. **167**, 550 (1946); Phys. Rev. **74**, 639 (1948).
[21]C. M. Wayman, in *Martensite Transformations,* Proceedings of the International Conference on Martensitic Transformations ICOMAT-89, Sydney, Australia, 1989, edited by B. C. Muddle (Trans Tech, Switzerland, 1990).
[22]G. V. Kurdjumov and A. G. Khachaturyan, Metall. Trans. **3**, 1069 (1972).
[23]A. G. Khachaturyan, Sov. Phys. Solid State **5**, 16 (1963); **5**, 548 (1963).
[24]A. G. Khachaturyan, Sov. Phys. Solid State **9**, 2249 (1968).
[25]H. E. Cook and D. de Fontaine, Acta Metall. **17**, 915 (1969).
[26]D. N. Hoffman, Acta Metall. **18**, 819 (1970).
[27]G. V. Kurdjumov and A. G. Khachaturyan, Acta Metall. **23**, 1077 (1975).
[28]G. V. Kurdjumov, Metall. Trans. **7A**, 999 (1976).
[29]X. Liu, F. Zhong, J. X. Zhang, M. X. Zhang, M. K. Kang, and Z. Q. Guo, preceding paper, Phys. Rev. B **52**, 9970 (1995).
[30]A. G. Khachaturyan, *Theory of Structural Transformations in Solids* (Wiley, New York, 1983).
[31]A. G. Khachaturyan and G. A. Shatalov, Acta Metall. **23**, 1089 (1975).
[32]H. Kanzaki, J. Phys. Chem. Solids **2**, 24 (1957).
[33]M. Hayakawa and M. Oka, in *Martensitic Transformations,* Proceedings of the International Conference ICOMAT-86, Nara, Japan, 1986 (the Japan Institute of Metals, Japan, 1987), p. 296.
[34]G. V. Kurdjumov, J. Iron Steel Inst. London **195**, 26 (1960).
[35]G. V. Kurdjumov and L. Y. Lyssak, J. Iron Steel Inst. London **156**, 29 (1956).
[36]S. Kajiwara, T. Kikuchi, and S. Uehara, in *Martensitic Transformations* (Ref. 33) p. 307.
[37]H. Ino, K. Umezu, S. Kajiwara, and S. Uehara, in *Martensitic Transformations* (Ref. 33), p. 301.
[38]A. L. Roitbourd and A. G. Khachaturyan, Fiz. Met. Metalloved. **30**, 1189 (1970).